11-2016

Failure Mechanism of Woven Roving Fabric/Vinyl Ester Composites in Freeze–Thaw Saline Environment

Elias Anis Toubia
University of Dayton, etoubia1@udayton.edu

Sadra Emami
University of Dayton

Donald A. Klosterman
University of Dayton, dklosterman1@udayton.edu

Original Research Article

Corresponding Author:

Elias A. Toubia, Department of Civil Engineering and Engineering Mechanics, University of Dayton, Ohio 45469, USA

Email: etoubia1@udayton.edu

Failure Mechanism of Woven Roving Fabric/ Vinyl Ester Composites in Freeze-Thaw Saline Environment

Elias A. Toubia

Department of Civil Engineering and Engineering Mechanics, University of Dayton, Ohio 45469, USA

Sadra Emami , Donald Klosterman

Department of Materials Engineering, University of Dayton, Ohio, 45469, USA

Abstract

This experimental study investigates the degradation mechanisms of a GFRP material commonly used in civil engineering applications. A substantial reduction in tensile, shear,

and compression properties is observed after 100 days of freeze-thaw cycling in saline environment (-20 ^{0}C to 20 ^{0}C). Nondestructive inspection techniques were progressively conducted on unexposed (ambient condition) and exposed (conditioned) specimens. The Dynamic Mechanical Analysis showed permanent decrease in storage modulus that was attributed to physical degradation of the polymer and/or fiber-matrix interface. This indicated the formation of internal cracks inside the exposed GFRP laminate. The 3D X-Ray tomography identified preferred damage sites related to intralaminar and interlaminar cracks. The ultrasonic C-scan and optical microscopy showed the nature of the damage and fibers fracture. The thermal cycling events degraded the matrix binding the warp and fill fibers, impairing the structural integrity of the cross-ply laminate. The result of this work could benefit a multi-scale durability and damage tolerance model to predict the material state of composite structures under typical service environments.

Key Words: Fiber, freeze-thaw, cycling, degradation, X-ray, ultrasonic, damage

1. Introduction

Glass Fiber Reinforced Plastic (GFRP) composites are extensively being used in civil engineering applications, namely, pedestrian bridges, piling bumpers, offshore and marine structures. These GFRP are fabricated by the Vacuum Assisted Resin Transfer Molding

process (VARTM) and commonly use low cost woven roving (WR) E-glass fibers infused with a Vinyl ester resin. Their end use applications require continuous exposure to thermal cycling conditions, and their in-service environment is generally combined with aqueous environment or sea-water exposure. In cold regions, ice chemicals and rock salts are frequently used on highway and pedestrian bridges for ice and snow removal. In the last two decades, several researchers investigated the freeze/thaw (F/T) cycling effects on composite materials [1-6]. Significant reduction in mechanical properties was reported when thermal cycling occurred in an aqueous environment [1-11]. When F/T is combined with salt water, two mechanisms will most likely occur. The first one is related to matrix cracking under thermal cycling, and the second by diffusion through the resin down to the fibers. Resin degradation, fiber-matrix de-bond and fiber stress corrosion were found to be the major failure mechanisms in GFRP when immersed in sea water [12]. Experimental data available in the literature related to woven roving GFRP under F/T and saline exposure reported limited combination of mechanical tests and nondestructive inspection (NDI) techniques. This study provides a full spectrum of mechanical testing progressively backed by several comprehensive NDI techniques to better understand damage initiation in similar construction. Based on a recent literature survey conducted by Sousa et al. [8], it was felt that a detailed root cause failure analysis is needed to assist in the development of a

mechanistic model based on experiment relating the material degradation to the observed loss in stiffness and strength. Understanding the cause, nature, and how damage is induced by the thermal cycling, one would be able to quantify the reduction and properly predict the structural performance of the woven roving GFRP construction. If such root cause failure analysis is properly investigated, specifically locating the size and orientation of the defects, then a valid multi-scale durability and damage tolerance model could be generated and implemented in any finite element software package to predict the material state of composite structures under typical service environments.

In this paper, GFRP laminates identical to existing field applications are fabricated and tested. Several mechanical tests are presented along with thermomechanical analysis to measure internal damage and degree of micro-damage in the GFRP laminate. State-of-the-art non-destructive inspection techniques are used to locate the size and preferred sites of the defects. This approach is detailed in the following sections and justifies the reduction observed in WR construction. In addition, the long term objective of this paper is to set the stage to develop an accelerated test method and provide additional experimental data that will enable engineers to predict the long term performance of composite structures in harsh environment.

2. Experimental Program

2.1 Materials

The materials employed in this experimental study consist of 6 layers of E-glass plain weave fabric (813 g/m2) reinforced with Derakane 610C-200 epoxy-vinyl ester resin (Ashland Inc.). This resin is currently being used in several infrastructure applications due to its durability, toughness, and fire resistance properties. It consists of a liquid blend of vinyl ester monomers in styrene, where the styrene content is approximately 40-50 wt%. Although this type of thermosetting polymer resin is often referred to in industry as an "epoxy vinyl ester" resin, it actually does not contain any reactive epoxy groups nor does it cure by the same polymerization mechanism as most epoxy resin systems. It is synthesized through the reaction of epoxy monomers with methacrylic acid, which replaces all the epoxide groups with methacrylate groups. This reaction leaves a carbon-carbon double bond (referred to as vinyl) on the ends of each monomer, which is attached to the main monomer through an ester linkage, thus the term "vinyl-ester". The main purpose of this is so that the polymerization can be initiated at room temperature with the use of peroxide-based initiator systems due to the reaction of peroxide with the carbon-carbon double bond. However, the presence of the ester group also allows for the increased possibility of

hydrolysis decomposition, compared to epoxy resin systems which do not contain the ester linkage.

The initiator system used was Cadox 50 at a level of an amount of 1.25 wt%. This material is primarily a solution of methyl ethyl ketone peroxide (MEKP). One large panel was fabricated using the vacuum assisted resin transfer molding (VARTM) at Composite Advantage LLC. (Dayton, Ohio). The panel was actually a sandwich core composite containing a PVC foam core, however, the laminate skins were cut away afterwards to supply a solid laminate sample for testing as the focus of this study. These molded cross-ply laminates were allowed to cure for 30 days under ambient conditions (23°C and 50% RH). Nominal properties of composite constituents are listed in Table 1. The fiber volume fraction was approximately 53% with a total measured laminate thickness of 3.24 ± 0.1 mm.

Table 1- Properties of Constituent Materials

Property	E-Glass fiber	Derakane 610C-200 vinylester- Resin
Tensile Strength (MPa)	3400	71
Tensile Modulus (GPa)	80	3.53
Elongation (%)	4.6	4.5

Density (g/cc)	2.62	1.07
Heat Distortion Temperature	-	76 ^{0}C

2.2 Environmental Exposure

All fabricated specimens were subjected to the following two exposure conditions:

a) Unexposed: Storage at room temperature (23°C and 50% RH)
b) Exposed: Exposure to freeze-thaw (F/T) with immersion in saline solution (100 days)

To simulate sea–water environment, the exposed samples were fully immersed in a solution of deionized water containing 3% NaCl (sodium chloride). The exposed samples were subjected to 100 days of accelerated F/T cycling tests. Each cycle consists of 12 hour period with a temperature range of -20 °C to 20 °C (Figure 1). A programmable freeze-thaw climate chamber (Slab Tester-Qualitest^{TM}) was used to thermally cycle all specimens for a total of 200 cycles (100 days).

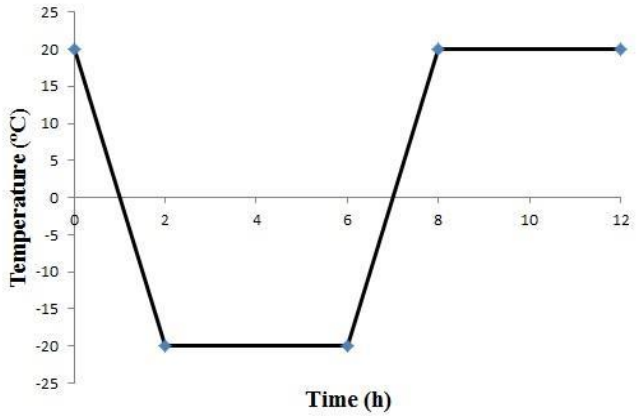

Figure 1- Freeze-Thaw Cycle Profile (12 hours period)

2.3 Mechanical Testing

After exposure, all specimens were paced under ambient condition and allowed to dry for 72 hours. A total of 48 test coupons were cut using a diamond table saw and prepared according to the ASTM procedures. Strain gages were installed on 3 exposed and unexposed samples for each standard test. Complete details of sample dimensions and number of samples are displayed in Table 2. Longitudinal and transverse direction strains were installed on the tensile test coupons. The V-notched beam test samples were mounted with strain gauges in the + 45 and – 45 degree directions on one side of each the test coupon.

Table 2- Composite Laminates Standard Evaluation Tests

Standard Test	**Nominal Dimensions length, width, thickness (mm)**	**Number of Samples Exposed/Unexposed**
Shear V-Notched Beam (ASTM D5379) IOSIPESCU	76.5×19×3.24	6 / 6
Laminate Tensile Test (ASTM D3039)	254×25.4×3.24	6 / 6
Laminate Compression Test (ASTM D6641)	139.7×6.35×3.24	6 / 6

2.4 Dynamic Mechanical Analysis (DMA), Differential Scanning Calorimetry (DSC), and NDE Testing

The effect of thermal cycling on the microstructure and physical properties of the polymer and laminates was characterized by Dynamic Mechanical Analysis (DMA) and Differential Scanning Calorimetry (DSC) techniques. The DMA unit was a TA Instrument Q800 operated in 3 point bending mode from 25-130°C at 5°C/min. The frequency of oscillation was 1 Hz and strain amplitude of TMA was used to obtain the glass transition temperature and the coefficient of thermal expansion (CTE). The operating parameters for this test were

25-130°C @ 5°C/min. Each sample (exposed and unexposed) was subjected to two heating cycles. The first cycle removed the non-reversible effects such as residual curing, stress relief etc. The second heat was used to extract information about the fully cured polymer.. DSC testing was performed on neat resin samples with a TA Instruments Q2000 from 40-250°C at 10°C/min, followed by cooling and reheating. Sample size was approximately 5-10 mg. The neat resin samples were cut from blocks of resin leftover from the VARTM process in the resin reservoir. Although the thermal history of the resin in the reservoir is usually not the same as experienced in the composite, at least the material can be used to study the effect of freeze-thaw on the resin independently of fibers. Ultrasonic C-Scan technique was employed to assess the damage in the laminates. An ultrasonic reflector plate (immersion reflection) with 5 MHz transducer frequency was applied on the test coupons, with a scan/index length of 381 mm and an increment of 0.51 mm. A 360 degree X-ray CT-scan inspection (X-Tek real time HMX160) was applied to map out and determine the internal damage after exposure. High Resolution Scanning Electron Microscope (HRSEM-Hitachi S-4800) was used to study the microstructure and defects in the woven roving (WR) structure. All DSC, DMA and NDE techniques were applied on exposed and unexposed panels (control panels). These test methods and results are discussed next.

3. Results and Discussion

Table 3 shows the average mechanical test results and Coefficient of Variations (COV) for each standard test (average of 12 samples per standard test). All mechanical characterization tests were conducted using a calibrated test machine (INSTRON 4208). The COV for strength and modulus for all specimens were less than 15.3 %.

Table 3- Mechanical Test results

Sample Type	Test	Direction	Average Modulus (GPa)	Modulus COV%	Average Strength(MPa)	Strength COV%
Unexposed	Shear	-	4.76	7.8	67.4	2.6
	Tension	Longitudinal	31.09	4.7	453.6	7.8
	Tension	Transverse	32.7	14.9	-	-
	Compression	Longitudinal	31.11	5.5	424.6	3.3
Exposed	Shear	-	3.87	9.6	58.3	6.8
	Tension	Longitudinal	24.9	4.91	347.14	12.85
	Tension	Transverse	30.2	15.3	-	-
	Compression	Longitudinal	27.7	2	352.2	9.6

Normalized moduli and strengths for shear, tension, and compression are shown in Figure 2. Large reductions occurred in the tensile and compressive strengths of the GFRP material. The shear and tensile longitudinal moduli were also reduced after F/T exposure. In general, the compression strength in WR fabric is lower than the tensile strength; this is due to the already kinked fibers; however this is not the case after exposure (Table 3, row 6 and 8). The tensile test results are mainly dominated by the fiber properties and clearly indicate that the longitudinal fibers and the structural integrity of the WR have been endangered due to the environmental conditions. A mechanistic model, which describes the mechanism of deterioration of the exposed laminates, is described in the root cause failure analysis section.

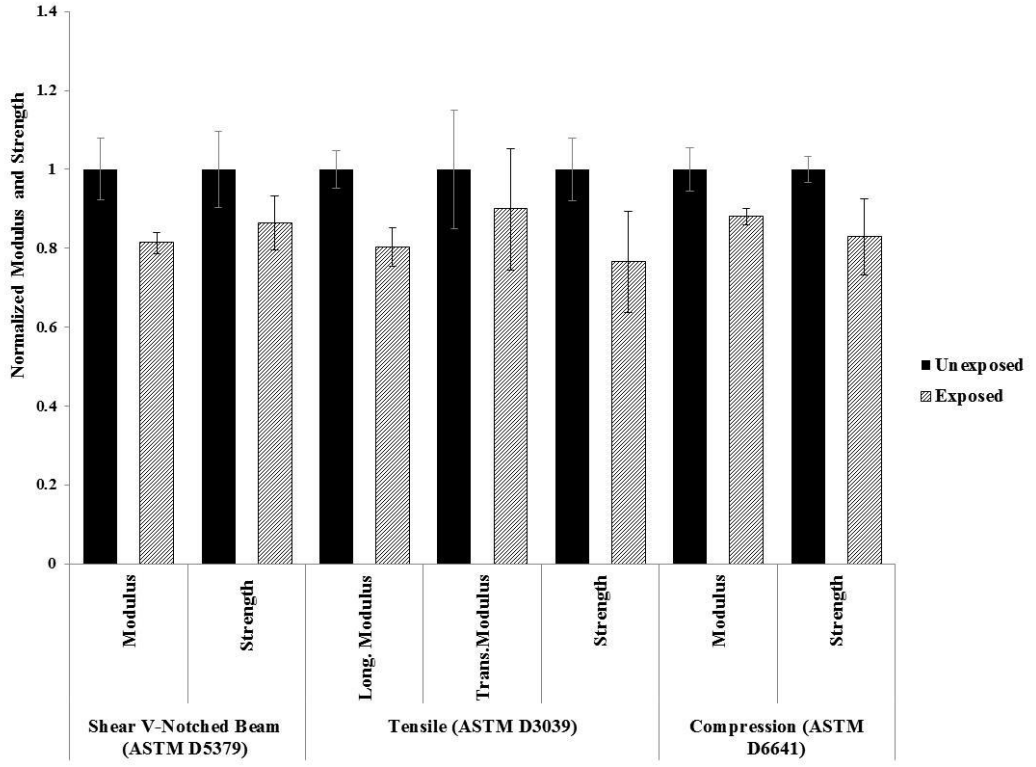

Figure 2- Overall results of exposed (200 cycles) and unexposed (0 cycle) specimens

3.1 Effect on Shear Properties

Effect of exposure on shear properties of the laminates was studied in accordance to the v-notched beam test (ASTM D5379-12) [13]. Figure 3 shows typical shear failure mode that occurred at the mid-span of the V-notched beam. The average reduction in shear modulus and strength after 100 days of exposure is 18.5% and 13.5 %, respectively (Figure 4).

Similar reductions were reported by Guzman and Brøndsted [12] after 8 years of salt water exposure.

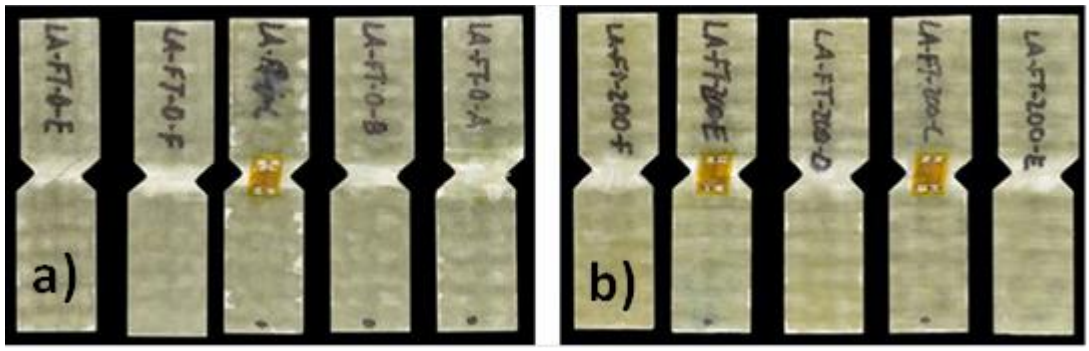

Figure 3- Shear failure modes for a) unexposed; and b) exposed specimens

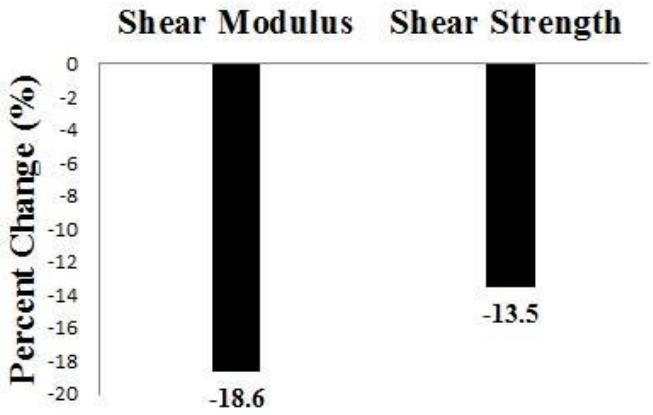

Figure 4- Percent change in shear modulus and strength

Following the shear test, failed samples were cut in between the V-notch locations (across the length of the sample) and dissected using an optical image technique. Figure 5 shows the final fracture states and internal cracks for the unexposed and exposed specimens. The unexposed failed specimens exhibited interlaminar cracks and separation in between the resin and warp fibers. The cracks were oriented along the warp direction. For the exposed failed samples, a high density of intralaminar cracks occurred along the fill fibers as well as their interfaces (Figure 5). This clearly shows that the resin has been degraded due to the F/T cycling.

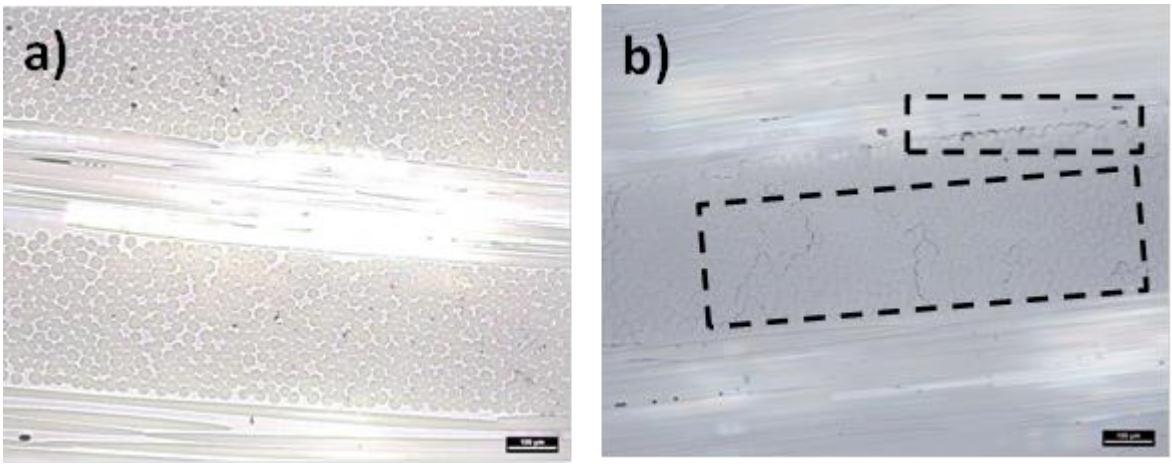

Figure 5– Micrograph of the cross section after failure at the V-notch location a) Unexposed: showing only interlaminar cracks, b) Exposed: showing interlaminar and intralaminar cracks

3.2 Effect on Tensile Properties

In this test a 23% reduction in the tensile strength and 19.7% in the longitudinal modulus occurred after exposure. These values are significantly higher than the COV listed in Table 3. Since the ASTM D3039 [14] test results are mainly dominated by the fibers, this presumably indicates that the fibers were damaged in the longitudinal and transverse directions of the WR construction. In general, when a delaminated composite material is subjected to tension, the residual strength is reduced by only 10 to 15 % [15]. Lateral strains (90 degree direction) were used to monitor and extract the stiffness of the laminate in the transverse direction. The transverse modulus decreased by 10 %. The failure modes are shown in Figure 7. It is interesting to note that Guzman and Brøndsted [12] reported similar reductions in transvers tensile modulus and strength (single glass fiber) after 8 years in salt water environment.

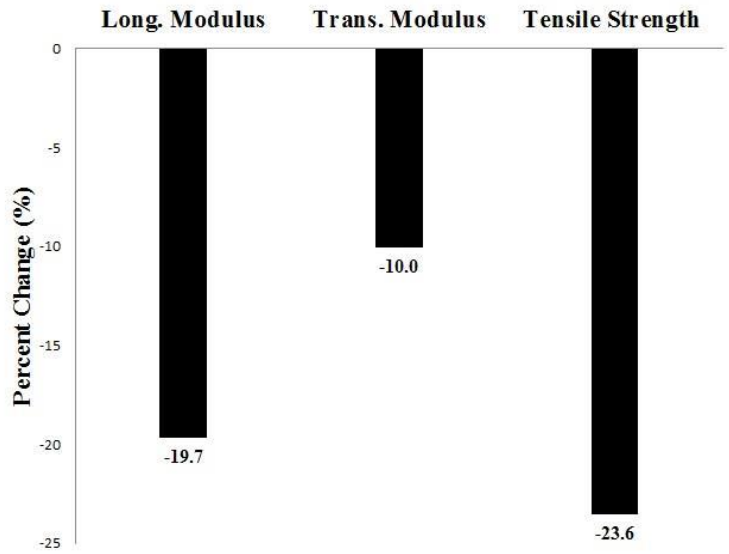

Figure 6– Percent change in tensile modulus and strength

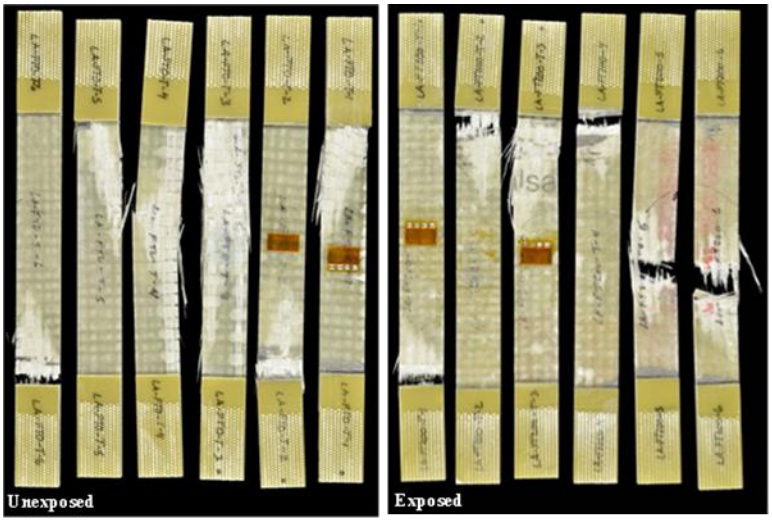

Figure 7– Tensile test failure modes; unexposed and exposed specimens

Figure 8 shows the tensile stress-strain curves in the longitudinal and transverses directions. For the exposed samples, the transverse strains are more pronounced than the unexposed samples. These highly deviated curves designate some sort of stiffness degradation due to loss in the structural integrity of the laminate, especially at the weave junctions (nodes) between the 0 and 90 degree fibers of the WR construction. This could be a direct result of a weakened matrix that binds the warp fiber to the fill fiber. More in-depth validation of this key failure mechanism is explained in the non-destructive testing section.

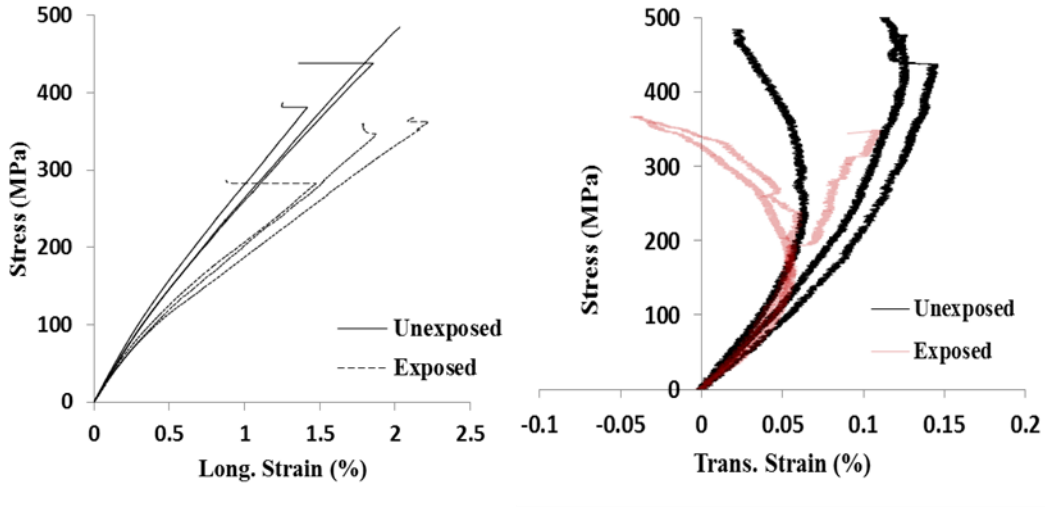

Figure 8- Longitudinal and transvers Stress-Strain curves for exposed and unexposed specimens

3.3 Effect on Compressive Properties

The combined loading compression test fixture was used to study the effect of exposure on the compressive properties of the GFRP laminates. A total of 12 samples were tested in accordance with ASTM D6641 [16]. The exposed samples showed an average reduction of 17.1% in strength and 12% in modulus. One can notice the high dependency of the matrix degradation and interfacial failure on the compression strength versus the shear strength observed in Figure 4. Typical experienced failure modes are shown in Figure 9.

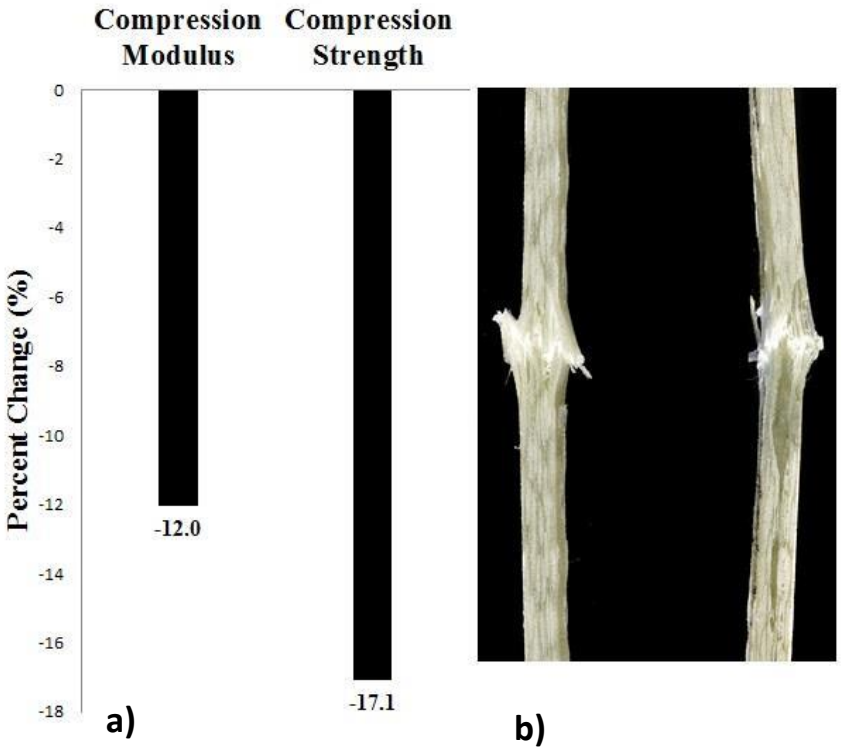

Figure 9 –a) Percent change in modulus and strength, b) Compression failure modes

3.4 Root Cause Failure Analysis

3.4.1 Dynamic Mechanical Analysis (DMA) and Differential Scanning Calorimetry (DSC)

To study the internal damage or defects that occurred due to these environmental conditions, a DMA and DSC tests were conducted on unexposed and exposed laminates.

The DMA results are given in Figure 10. Figure 10a shows the results obtained from the 1st heating cycle (25-140°C @ 5 C/min). After cooling the sample in the apparatus, a 2nd heating cycle was run on the same specimen. The reheat cycle results (Figure 10B) show the condition of the material after being post cured. This analysis is commonly run for thermosets because usually they are not fully cured in the original manufacturing process.

Polymers generally are viscoelastic materials, exhibiting simultaneous elastic and viscous behavior in response to time varying stress. The amount of each type of behavior depends on the state of the polymer structure (chemical composition, crosslink density) and the temperature. The storage modulus (E') characterizes the elastic energy stored by the polymer, while the loss modulus (E") represents the energy lost to viscous dissipation. Polymers that are highly crosslinked usually have high values of E'. Also, the shape of the E' and E" curves can be used to locate the temperature at which the polymer structure

transitions from a glassy state (at low temperature) to a rubbery state (at higher temperature).

Referring to Figure 10a, the sample subjected to 200 freeze-thaw cycles exhibited a 20% decrease in E' near room temperature. This could be due to a variety of reasons, such as plasticization of the matrix, chemical decomposition of the matrix, physical degradation of the fiber-matrix interface, etc. Chemical decomposition of the matrix could be explained by hydrolysis of the ester linkage in the vinyl ester matrix, although hydrolysis reactions usually slow at the temperatures encountered. Therefore, the change may be due to physical degradation of the resin and/or fiber-matrix interface from the freeze-thaw exposure.

The E" curves provide more information about the phase structure of the resin. Cured vinyl ester resins usually are comprised of two polymers phases: 1) the main crosslinked structure which is comprised of the vinyl ester – styrene copolymer network, and 2) a phase rich in homopolymerized linear polystyrene. The peaks in the E" curve correspond to the temperature at which each phase transitions from glassy to rubbery state. The glass transition of polystyrene is approximately 100°C, which corresponds closely with "phase 1" peak. The glass transition of the copolymer network is generally observed to be higher: in this case it occurs at 115°C, and is labeled as "phase 2" in the 0-cycle sample. It is

interesting that the 200-cycle sample does not exhibit the phase 2 transition in the same location. Most likely, the phase 2 transition was reduced to about 75°C (labeled as phase 2', which is the shoulder in the E" curve, as well as the steep drop in E'). Absorbed water would be expected to plasticize the main network because it has some polarity (e.g. ester bonds), while water should have little or no impact on the highly nonpolar polystyrene phase. Indeed, the phase 1 peak is almost identical in both samples.

Figure 10B shows the results after post curing the samples. Any water in the matrix is expected to be removed in the 1st heating cycle. The value of E' for the 200-cycle sample remained lower (17.5%) than the control sample, which indicates that there was some nonreversible degradation caused by the freeze-thaw cycles. The E" peak of the polystyrene phase (phase 1) was largely unaffected by the post curing process in both 0 and 200 cycle samples. In the 0 cycle sample, the E" peak of the vinyl ester phase shifted to a slightly higher temperature (120°C), which can be attributed to residual curing from the 1st heating cycle. In the 200 cycle sample, the vinyl ester E" peak is seen as a faint shoulder around the same temperature as the 0 cycle sample. This indicates that the vinyl ester network was no longer plasticized, but was not as prevalent as the 0 cycle sample. As with the E' result, this also indicates some difference in the network or fiber-matrix interface caused by the freeze-thaw cycle.

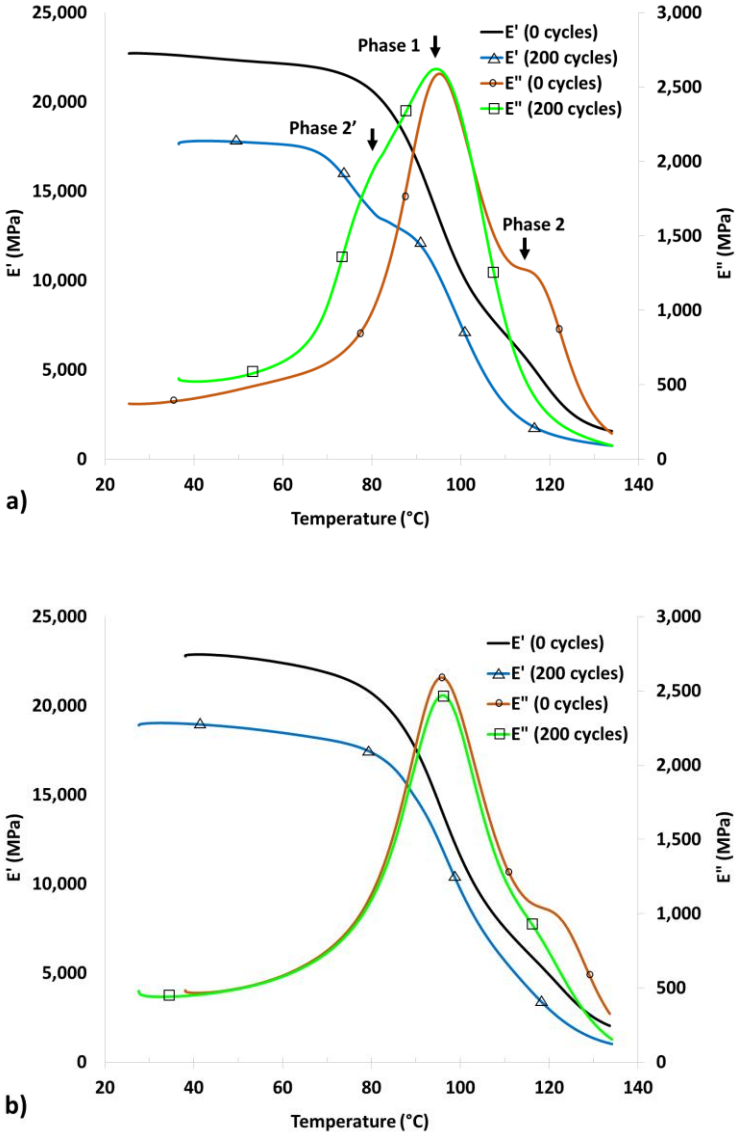

Figure 10: DMA results for composite, a) 1st DMA heating cycle, b) 2nd DMA heating cycle.

The DSC results for a neat resin samples are summarized in Table 4. This technique was used to verify that the samples were not fully cured after VARTM processing, and to measure the T_g of the resin independently of the presence of fibers. The T_g is strongly related to the nature of the crosslinked network, and therefore it can provide information about the decomposition of the polymer. The DSC traces for the 1st heat showed a T_g around 67°C for the 0-cycle sample and 63°C for the 200-cycle sample. This difference was attributed to plasticization of the matrix from the freeze-thaw cycle, as observed in DMA. However, upon reheating the T_g increased to essential the same value (96-97°C) in both cases, due to post curing experienced in the prior cycle. This implies that there was no permanent chemical decomposition of the polymer, for example by hydrolysis. The permanent damage detected by DMA (drop in storage modulus) is therefore attributed primarily to *physical* degradation in the polymer (cracks) and/or between the polymer and fiber. The small change to phase 2 detected by DMA is not able to be detected by DSC.

Table 4: Summarized Tg Results from DSC.

# cycles	Tg (°C)	
	1st heat	2nd heat
0	68.0	96.3

	66.5	-
200	62.4	97.4
	64.3	-

3.4.1 Damage State in Woven Roving Architecture

In order to investigate the size and location of the internal defects, a 3D X-Ray CT-Scan test was conducted on the exposed specimens. Figure 11 shows resin cracking at preferred sites. In addition, intralaminar cracks occurred in the mid-section of the FRP laminate, specifically in resin rich areas. The damage shown in Figure 11 (transverse cross section) is approximately 1.2 mm in length and 0.7 mm thick. These defects (cracks and fractures) are source of delamination initiation that further degrades the component strength and eventually lead to local stiffness reduction.

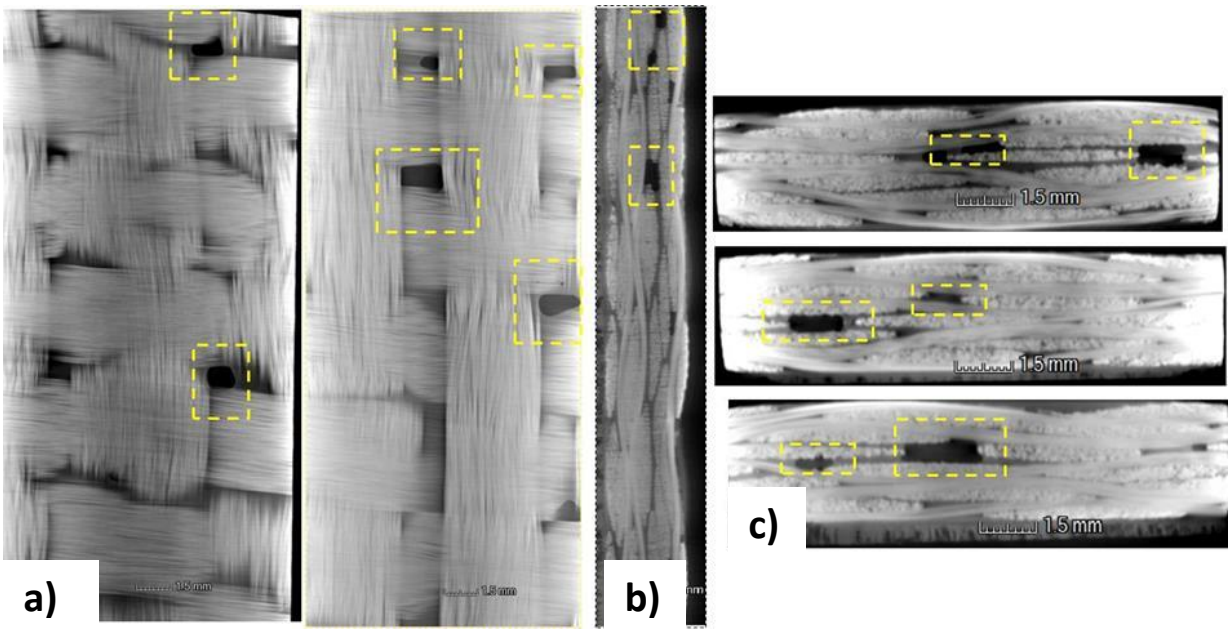

Figure 11- X-Ray computed tomography showing damage in exposed samples a) 2 nd and 3 rd plies, b) longitudinal cross section, c) transverse cross section

In order to test the structural integrity of the connections between the fill and warp fibers, a pulse ultrasonic C-scan technique was performed on two exposed and unexposed specimens. Figure 12 shows the C-scan images of all tested samples. The grid pattern (signals at nodes) is clearly shown in the unexposed samples (Figure 12a), whereas the linear pattern is clearly visible in the exposed samples. This change in pattern indicates that these connections are impaired and ineffective in transferring the loads, including racking or shear loads. In addition to the shear stiffness loss of the cracked matrix, the deterioration

of these nodes is believed to affect the tensile and shear moduli of the laminate. To interpret this phenomenon, one could envision the laminate structure similar to a picture frame (hinged truss) with some degree of rotational stiffness at the four pins (nodes). Two of these pins could be connected with a horizontal spring simulating the lateral stiffness supplied by the matrix. If a load (tension of shear) is applied to the truss, the capability of the truss to resist load and deformation (axial or racking) is controlled by the rotational stiffness supplied by the nodes (bond at junction of fill and warp fibers) and the axial stiffness of the spring. This simple mechanistic model helps to understand the basic phenomena governing the behavior of these systems.

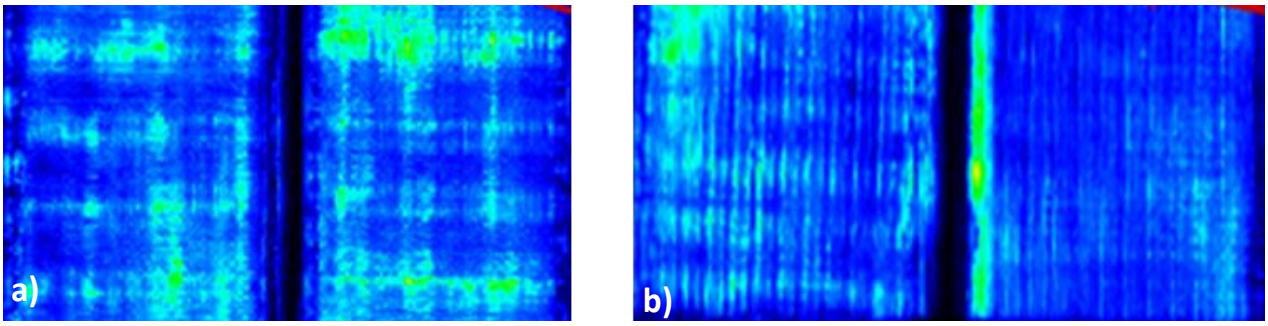

Figure 12- Ultrasonic C-scan results (102 mm wide specimens); a) unexposed: grid pattern, b) exposed: linear pattern

3.4.2 Matrix and Fiber Damage

To map out the damage and frequency of defects that occurred in the laminate after exposure, a high resolution optical image technique was used to inspect their locations. Figure 13 shows damaged fibers and matrix bond failure between the fill and warp fibers. This failure pattern commonly occurred at the kink/weave location between the roving. It seems that the volume change due to the thermal cycling initiated a high non-uniform residual stresses at the sharpest curvature location and significantly degraded this node/junction between the fibers. The authors believe that this damage will be recurrent for any plain weave type no matter what type of reinforcement is used.

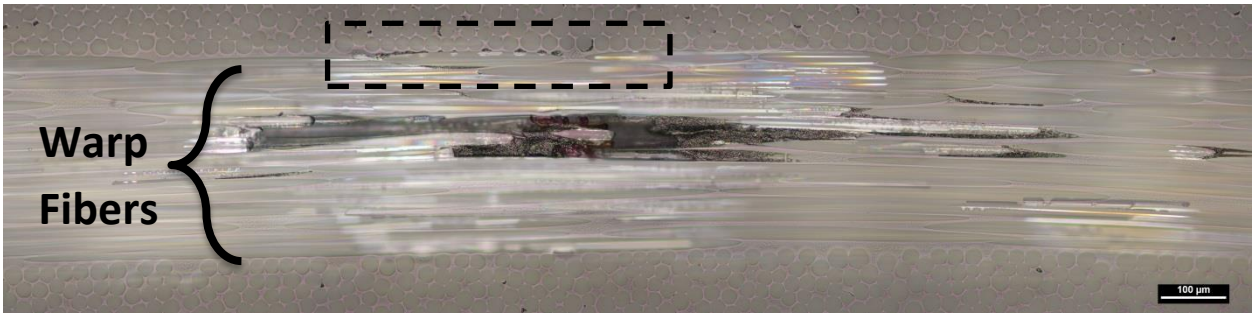

Figure 13- Local magnified optical image at weave junction showing matrix failure between damaged warp fibers and fill fibers after exposure

Figure 14 shows the microstructure of an exposed specimen with a high resolution Scanning Electron Microscopy (SEM). Significant amount of fiber/matrix degradation is observed. This justifies the DMA result discussed in section 3.4. The mismatch in the coefficient of thermal expansion between the resin and the E-glass fiber is believed to cause this interfacial failure mode. In addition, fiber fractures are clearly shown in Figure 14.

Figure 14– SEM micrograph showing degradation of fiber/matrix interface and fiber fracture

Karbahari et. al. [11] reported that aqueous solution in contact with glass fiber surface produced free-alkali hydroxide groups that degraded the silica structure of the glass fiber

when exposed to an alkaline media. The effect is through breaking of Si-O bonds in the glass network and was believed that surface loss and pitting occurred in areas of high pH solution. In general, alkali solution such as cement environment is known to degrade the glass fiber through several processes such as pitting, etching, leaching, and embrittlement [17-19]. Figure 15 shows a surface of a filament of glass fiber in an exposed sample. Several defects (black spots) are observed, including localized areas around these spots, which might be related to coupling agent or polymer swelling

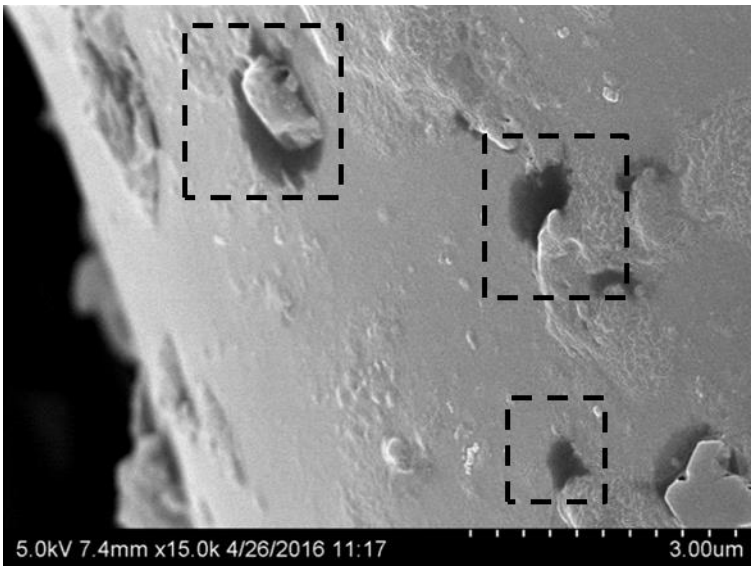

Figure 15- SEM picture of damaged E-glass fiber after exposure

4. Conclusion

This study presents the experimental results and evaluation of a woven roving E-glass fabric/ epoxy vinyl ester composite submerged in saline solution and exposed to 100 days of freeze-thaw environment. State-of-the-art NDI testing techniques were used to investigate the nature of the degradation, including all constituent materials, interfaces, and fabric construction. A mechanistic model describing the failure mechanism and damage initiation and propagation as related to observed material degradation and reduction is presented.

The following conclusions may be drawn:

1. The conditioned specimens showed a substantial material degradation when compared to identical control specimens. The largest reduction was observed in the tensile properties of the GFRP. A reduction of 23 % in strength and 20 % in modulus were detected. The average reductions in shear modulus and strength were around 18.5% and 13.5%, respectively. Whereas an average reduction of 17.1% in compression strength and 12% in compression modulus were observed.

2. The shear failure postmortem optical microscopy images showed delamination and intralaminar cracks in the exposed samples.
3. The DMA testing indicated plasticization of the matrix from the exposure. The plasticization effects could be removed by heating the sample (thereby removing water) but there was a permanent decrease in storage modulus that is attributed to physical degradation of the polymer and/or fiber-matrix interface. Most likely hydrolysis of the resin was not involved. DSC results corroborated these findings. These results are consistent with the formation of internal cracks inside the GFRP laminate.
4. The fiber/matrix interface has traditionally been viewed as the main damage due to thermal cycling. However, when F/T is combined with saline exposure, the warp fibers specifically at the weave junctions experienced extensive damage and fracture.
5. The X-ray computed tomography showed a preferred site location of defects in the woven roving construction. The frequency of these defects was mainly located in the resin rich areas between the fill and warp fibers.
6. The ultrasonic C-scan and optical microscopy showed that the volume change due to F/T cycling and reduction of through-thickness tensile strength of the matrix

binding the warp and fill fibers at the weave junction impaired the structural integrity of the FRP material.

7. The observed strength and stiffness reductions after accelerated exposure were similar to what was reported in the literature [12] on GFRP immersed in sea water for up to 8 years. The testing scheme and protocol proposed in this study could be used as an accelerated testing method for future evaluation of durability in composite materials.
8. The results of this research are expected to apply to plain weave fabric regardless of the fiber types used in the reinforced polymer composites. A multi-scale durability and damage tolerance model would take advantage of the damage types presented in this paper, including the frequency, sizes, shapes, locations and distribution of the defects.

Acknowledgment

The Authors would like to acknowledge the assistance of our colleagues from the University of Dayton Research Institute, Ms. Mary Galaska for conducting the DMA testing, Ms. Marlene Houtz for the X-Ray computed tomography testing, Dr. Dale Grant and Carl-william O Sjoblom for SEM and optical microscopy, and Dr. Ray Kao for ultrasonic pulse testing. The composite panels were molded by Composite Advantage LLC.

Funding

This research received no specific grant from any funding agency in the public, commercial, or not-for-profit sectors.

References:

1- Rivera J, Karbhari VM. Cold-temperature and simultaneous aqueous environment related degradation of carbon/vinylester composites. *Composites Part B: Engineering*. 2002 Jan 31; 33(1):17-24.

2- Shi JW, Zhu H, Wu G, Wu ZS. Tensile behavior of FRP and hybrid FRP sheets in freeze–thaw cycling environments. *Composites Part B: Engineering*. 2014 Apr 30; 60:239-47.

3- Gomez J, Casto B. Freeze-thaw durability of composite materials. *First International Conference on Composites in Infrastructure*. 1996 Jan.

4- Wu HC, Fu G, Gibson RF, Yan A, Warnemuende K, Anumandla V. Durability of FRP composite bridge deck materials under freeze-thaw and low temperature conditions. *Journal of bridge engineering*. 2006 Jul; 11(4):443-51.

5- Lord HW, Dutta PK. On the design of polymeric composite structures for cold regions applications. *Journal of Reinforced Plastics and Composites*. 1988 Sep 1; 7(5):435-58.

6- Marouani S, Curtil L, Hamelin P. Ageing of carbon/epoxy and carbon/vinylester composites used in the reinforcement and/or the repair of civil engineering structures. *Composites Part B: Engineering*. 2012 Jun 30; 43(4):2020-30.

7- Aniskevich K, Aniskevich A, Arnautov A, Jansons J. Mechanical properties of pultruded glass fiber-reinforced plastic after moistening. *Composite Structures*. 2012 Sep 30; 94(9):2914-9.

8- Sousa JM, Correia JR, Cabral-Fonseca S, Diogo AC. Effects of thermal cycles on the mechanical response of pultruded GFRP profiles used in civil engineering applications. *Composite Structures*. 2014 Oct 31; 116:720-31.

9- Dutta PK, Hui D. Low-temperature and freeze-thaw durability of thick composites. *Composites Part B: Engineering*. 1996 Dec 31; 27(3):371-9.

10- Wu L, Murphy K, Karbhari VM, Zhang JS. Short-term effects of sea water on E-glass/vinylester composites. *Journal of applied polymer science*. 2002 Jun 28;84(14):2760-7.

11- Karbhari VM, Chu W. Degradation kinetics of pultruded E-glass/vinylester in alkaline media. *ACI materials journal*. 2005; 102(1):34-41.

12- Guzman VA, Brøndsted P. Effects of moisture on glass fiber-reinforced polymer composites. *Journal of Composite Materials*. 2014 Mar 13:0021998314527330.

13- ASTM, D5379/D5379M-05. *Standard test method for shear properties of composite materials by the V-notched beam method*. West Conshohocken, PA: American Society for Testing and Materials, 2005.

14- ASTM, D3039/D3039M-08. *Standard test method for tensile properties of polymer matrix composite materials*. West Conshohocken, PA: American Society for Testing and Materials, 2008.

15- Heslehurst RB. Defects and Damage in composite materials and structures. *CRC Press*; 2014 Apr 21.

16- ASTM, D6641/D6641M-09. *Standard test method for compressive properties of polymer matrix composite materials using a combined loading compression (CLC) test fixture*. West Conshohocken, PA.: American Society for Testing and Materials, 2009.

17- Bank LC, Puterman M, Katz A. The effect of material degradation on bond properties of fiber reinforced plastic reinforcing bars in concrete. *ACI Materials Journal*. 1998 May 1; 95:232-43.

18- Sen R, Mullins G, Salem T. Durability of E-glass/vinylester reinforcement in alkaline solution. *ACI Structural Journal*. 2002 May 1; 99(3):369-75.

19- Yilmaz VT. Chemical attack on alkali-resistant glass fibers in a hydrating cement matrix: characterization of corrosion products. *Journal of non-crystalline solids*. 1992 Dec 2; 151(3):236-44.